Progress In Electromagnetics Research M, Vol. 107, 79–89, 2022

X-Band Multilayer Butler Matrix and SIW Multi-Beam Antenna: Analysis and Design

Moustapha Mbaye, Larbi Talbi, Siwar Louati, Khelifa Hettak, and Halim Boutayeb*

Abstract—This article presents a new Butler matrix made on stacked Printed Circuit Boards (PCBs). The matrix is based on Substrate Integrated Waveguides (SIW) and microstrip lines. Transitions using through metallic vias are designed and optimized for the crossover sections of the matrix. The other components of the circuit are as follows: 3-dB SIW directional coupler, 45° phase-shifter, and SIW dual-slot linear antenna array. Different sections of the matrix were simulated, fabricated, and tested. Using the full structure with radiating elements, we obtained good numerical and experimental results in terms of radiations patterns for the different beam directions, impedance matching, and isolation between the input ports.

1. INTRODUCTION

In nowadays wireless communication systems, Multi-Beam Antennas (MBAs) have become essential because of their ability to reduce undesirable interferences and thus to improve the quality of communication. An MBA is usually made of a Beam Forming Network (BFN) [1]. Beamforming networks can be used for Space Division Multiple Access (SDMA) [2] and multi-port amplifiers for distributed amplification in satellite systems [3]. Since the early 1960s, two families of beam forming networks have been proposed: quasi-optic designs and circuit designs. The quasi-optic designs include boot-lace lenses such as Ruze and Rotman lenses, which usually suffer from low efficiency due to spillover and high coupling losses among adjacent ports. These make quasi-optic designs less appropriate for high power applications [4–6]. Circuit beam forming networks, based on various guided-wave transmission lines such as directional couplers, crossover lines, and phase-shifters, are available in the literature, for example, the Blass matrix [7], Nolen matrix [8], and Butler matrix [9].

The Butler matrix is the most used beam forming network. It has theoretically low loss, employs the least number of components [10], and requires far fewer phase shifters than the Blass and Nolen matrices. However, the main challenges in the Butler matrix are the design of the crossover and the difficulty to obtain good phase characteristics. Various designs were proposed in [11–15] by using Substrate Integrated Waveguides (SIWs) and with solutions for omitting the crossover and for improving the phase balance compared with the traditional Butler matrix. The solutions presented in [11] increases the size of the matrix, and miniaturization techniques are proposed in [12–15]. Stacked Printed Circuit Boards (PCBs) and coupling slots are used in [13], whereas multilayer PCB technology is used in [15].

In this paper, a new multilayer 4×4 Butler matrix with microstrip lines, SIW couplers, and SIW phase shifters is proposed for X-band applications. The main novelty of our design is the utilisation of low cost stacked PCBs with metallic wires transitions for the crossovers. The different sections of the matrix are tested independently. The full structure is implemented, fabricated, and tested. A

Received 14 October 2021, Accepted 16 December 2021, Scheduled 10 January 2022
* Corresponding author: Halim Boutayeb (halim.boutayeb@uqo.ca).
The authors are with the Department of Electrical Engineering, University of Quebec, 101 rue Saint-Jean Bosco, Gatineau (Qc) J8X 3X7, Canada.

multi-beam antenna is also designed and tested by using the proposed matrix with a SIW antenna array.

The remainder of the paper is organized as follows. Section 2 describes the design and tests of the different components of the proposed matrix. Then, numerical and experimental results are presented for the full matrix in Section 3. Section 4 presents the SIW antenna array, and Section 5 gives the result for the optimized multi-beam antenna. Finally, concluding remarks are given in Section 6.

2. DESIGN AND TESTS OF THE DIFFERENT COMPONENTS OF THE BUTLER MATRIX

The schematic of a multilayer 4×4 symmetric Butler matrix can be represented as shown in Fig. 1. The matrix consists of 3-B 90° directional couplers, 45° phase shifters, and crossovers.

In the rest of this section, and in all the paper, an electromagnetic solver based on the finite element method (Ansys HFSS) has been used for the simulations and optimizations of the structures. A Rogers RT/Duroid 5880 is used as a substrate with permittivity (ε_r) of 2.2, height (b) of 0.508 mm, and $\tan\delta = 0.0009$. All S parameters measurements have been taken using the Agilent E8362B vector network analyzer.

A conventional waveguide is first optimized and then transformed to its SIW counterpart with the following design rules (via hole diameter d is 1 mm, and pitch size p is 2 mm), as reported in [16].

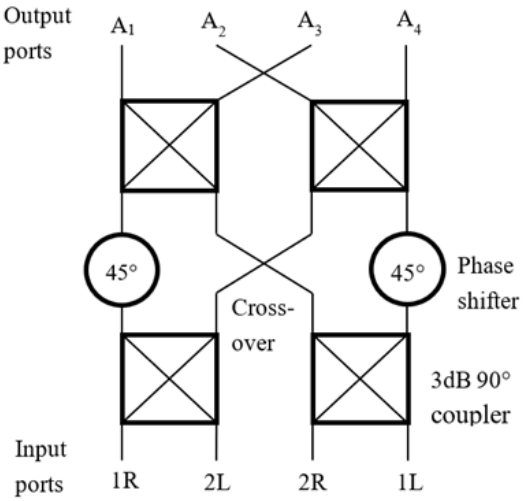

Figure 1. Schematic of a 4×4 Butler matrix.

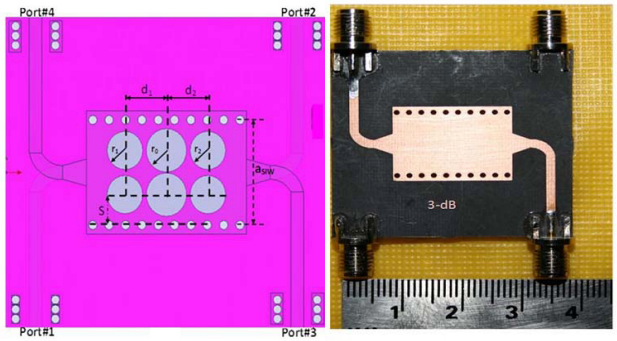

Figure 2. SIW based 3 dB 90° directional coupler. (a) Layout of the structure. (b) Photograph of prototype.

2.1. Double-Layer 3-dB SIW Directional Coupler

A double-layer SIW based 3 dB directional coupler as shown in Fig. 2 is proposed. The coupler is made of two SIW waveguides with three pairs of circular apertures located on the common wall. The two PCBs consisting of SIW waveguides are stacked together on the side of etched circular apertures as a common wall. The rows of circular apertures are used to couple the two SIW structures. Port 1 is the input-port; the direct output port is port 2; the coupled-port is port 3; and port 4 is used as an isolation port. The optimized design dimensions of the SIW coupler are (Fig. 2(a)) $a_{\mathrm{SIW}} = 12.1$ mm, $d_1 = d_2 = \lambda_g/4 = 5.13$ mm, $r_0 = 2.5$ mm, $r_1 = r_2 = 2.2$ mm, and $S = 3.3$ mm. Several steps of optimization were required to achieve the desired coupling without affecting the size of the structure. These steps are reported in Table 1.

The simulated and measured S-parameters of the proposed SIW directional coupler are shown in Fig. 3. From the curves in Fig. 3(a), the amplitude of the measured coupling factor (S_{31}) is around

Table 1. Optimized parameters for different coupling levels.

Number of apertures	r_0 (mm)	r_1 (mm)	r_2 (mm)	Offset (S) (mm)	Coupling value at 10 GHz
1	1.43			2.75	25 dB
1	2.525			2.84	19.2 dB
2 (in series)	2.525	2.425		2.92	16.3 dB
3 (in series)	1.5	2	2	3.0	15 dB
6 (3-3 in parallel)	2.5	2.2	2.2	3.3	3.7 dB

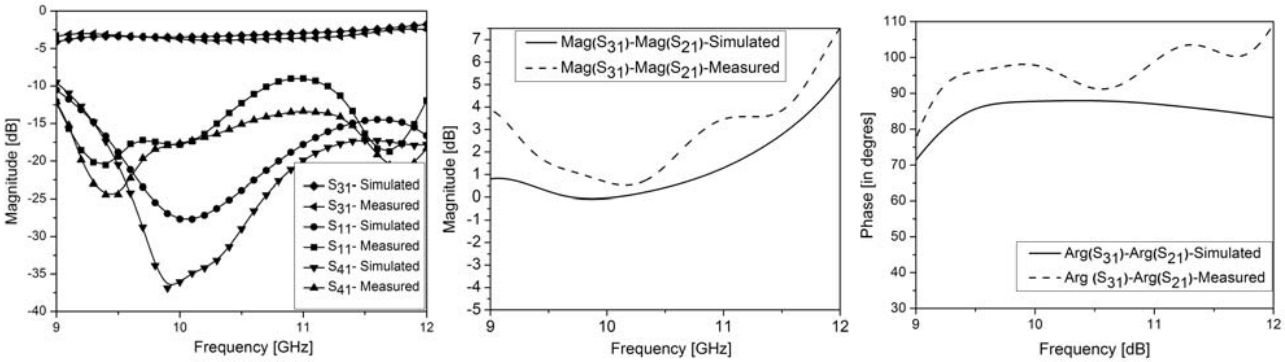

(a) (b) (c)

Figure 3. Simulated and measured S-parameters for the two-layer SIW hybrid coupler. (a) Magnitudes of coupling (S_{31}), reflection (S_{11}), and isolation (S_{41}). (b) Difference between the magnitudes of the transmission coefficients from port 1 to the direct (S_{21}) and coupled (S_{31}) ports. (c) Phase difference between the direct (S_{21}) and coupled (S_{31}) ports.

-3.7 dB which is in close agreement with the simulated result, i.e., -3.4 dB. The return loss S_{11} is well below the -18 dB over the operating frequency and is below -10 dB from 9 GHz to 12 GHz. The magnitude of S_{41} is below -15 dB over that frequency range. Fig. 3(b) shows the comparison of measured and simulated differences between magnitudes of S_{21} and S_{31}. It can be observed that it varies within 7.5 dB, and it is around 0 dB at 10.2 GHz. The phase difference between S_{21} and S_{31} is shown in Fig. 3(c). Its range variation is about 20°, and it is close to 90° from 9.5 GHz to 12 GHz. The oscillating effect observed with the phase is due to the nonlinear phase characteristics of the SIW based microstrip transition. These results show that the relative bandwidth of the 3-dB directional coupler is approximately 30%.

2.2. 4 Port through Via Transition Circuit

A new two-layer microstrip 4 port via-transition is presented in this section (Fig. 4). This transition consists of a low-loss interconnect between the two layers of the Butler matrix across two metallic wires. For ports 1 and 2, two-transmission lines on two layers share a common wall with a narrow transverse aperture across one via-transition. The same applies to ports 3 and 4.

With notations defined in Fig. 4 and this two-layer vias-transition, the incoming signal at port 1 is directly fed towards the output port 2 through one via, and the incoming signal at port 4 is directed towards output port 3 using another via. A clearance is made on the common broad wall to couple energy between ports 1 and 2. Another one is made to couple energy between ports 3 and 4 (as shown in Fig. 4(b)). The diameter of the aperture (D_{aperture}) is larger than the diameter of via (D_{via}) and must be optimized for good matching. The optimized dimensions are $W = 1.544$ mm, $D_{\min} = 4$ mm,

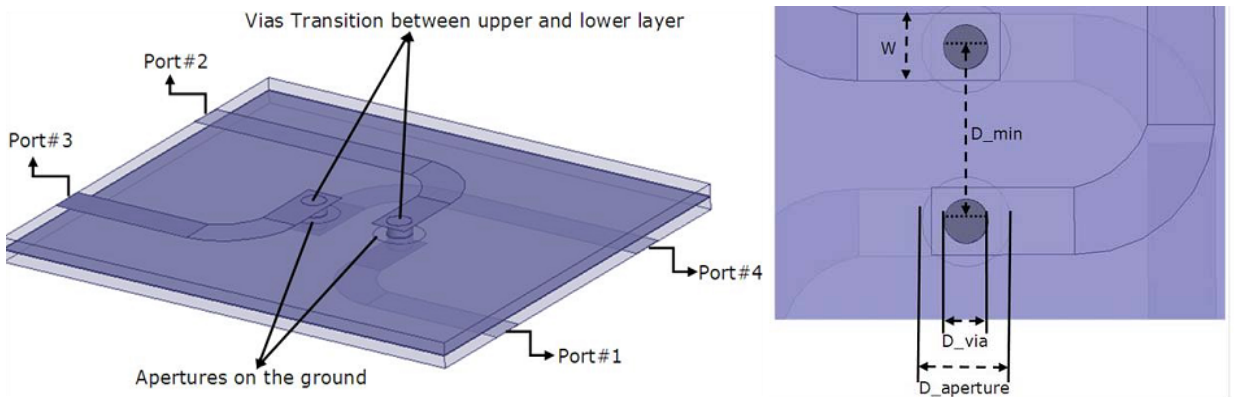

Figure 4. Two-layer microstrip 4 port via-transition. (a) 2D view of the structure. (b) Magnified vias-transition.

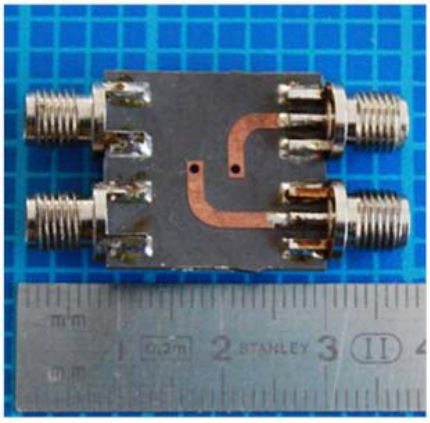

Figure 5. Photograph of the fabricated crossover element.

$D_{\text{aperture}} = 2.064\,\text{mm}$, and $D_{\text{via}} = 1.016\,\text{mm}$ as shown in Fig. 4(b). The fabricated prototype in shown in Fig. 5. Simulated and measured S-parameters for the proposed crossover are presented in Fig. 6. The isolation between input ports 1 and 3, as well as between the input and crossover output ports 1 and 4, is below $-30\,\text{dB}$ over the bandwidth of 8 GHz–12 GHz. The magnitude of S_{11} is below $-20\,\text{dB}$ over the same frequency band. The transmission coefficient obtained from port 1 to port 2 is around $-0.2\,\text{dB}$ over the desired bandwidth which indicates a small insertion loss.

2.3. 45° Phase Shifter

The proposed SIW phase shifter is designed based on the rules proposed in [16]. This structure, as shown in Fig. 7, is composed of two parallel arrays via holes, two metallic parallel plates, and two asymmetrical metallic posts. The parallel plates form the waveguide for signal transmission, and the locations of the asymmetrical posts in the substrate are used to control the phase of the wave. The optimized dimensions of the phase shifter are $a_{\text{SIW}} = 12.5\,\text{mm}$, $p = 2\,\text{mm}$, and $d = 1\,\text{mm}$. The positions of the two inserted posts with a diameter of 0.4 mm in the SIW waveguide are given in Table 2.

A prototype of the proposed 45° phase shifter was fabricated with a microstrip to SIW transition. This transition is composed of a tapered microstrip line (with a characteristic impedance Z_0) connecting to the SIW waveguide. The taper is designed to transform the quasi-TEM mode of the microstrip line into a TE_{10} mode in the waveguide. The optimized dimensions for the tapered transition are

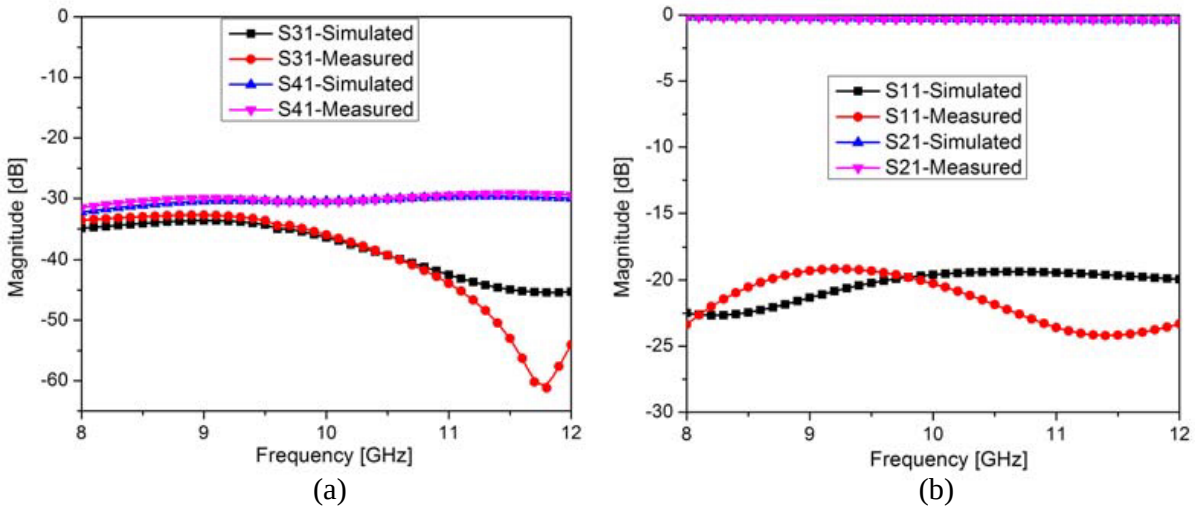

Figure 6. Simulated and measured S-parameters of the microstrip 4 port via-transition (a) isolation, (b) magnitudes of S_{11} and S_{21}.

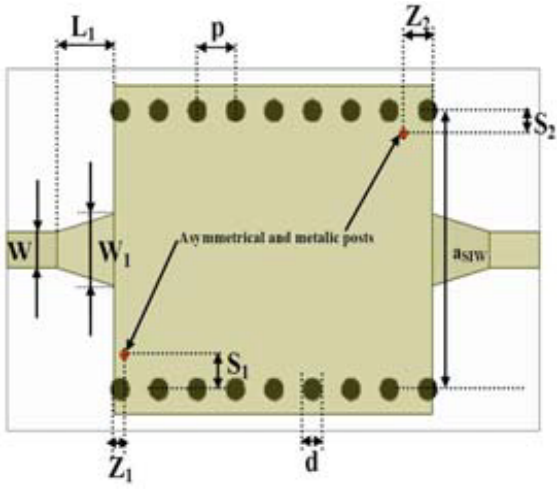

Figure 7. Proposed 45° phase shifter with two asymmetrical posts.

Table 2. Positions of the two inserted posts in the SIW.

Post 1		Post 2	
S_1	1.5 mm	S_2	0.5 mm
Z_1	0.5 mm	Z_2	1.5 mm

$W = 1.544$ mm, $W_1 = 3.08$ mm, and $L_1 = 3$ mm.

The magnitude and phase responses of the 45° phase shifter are presented in Fig. 8. The simulated and measured insertion losses at 10 GHz are about -0.1 dB and -1.1 dB, respectively. The simulated and measured phases at 10 GHz are about 45.37° and 45.8°, respectively. The measured phase curve is slightly shifted to higher frequency than simulation. The difference in insertion loss (S_{21}) may be attributed to tolerances of the substrate material, in terms of dielectric constant and conductor and dielectric losses.

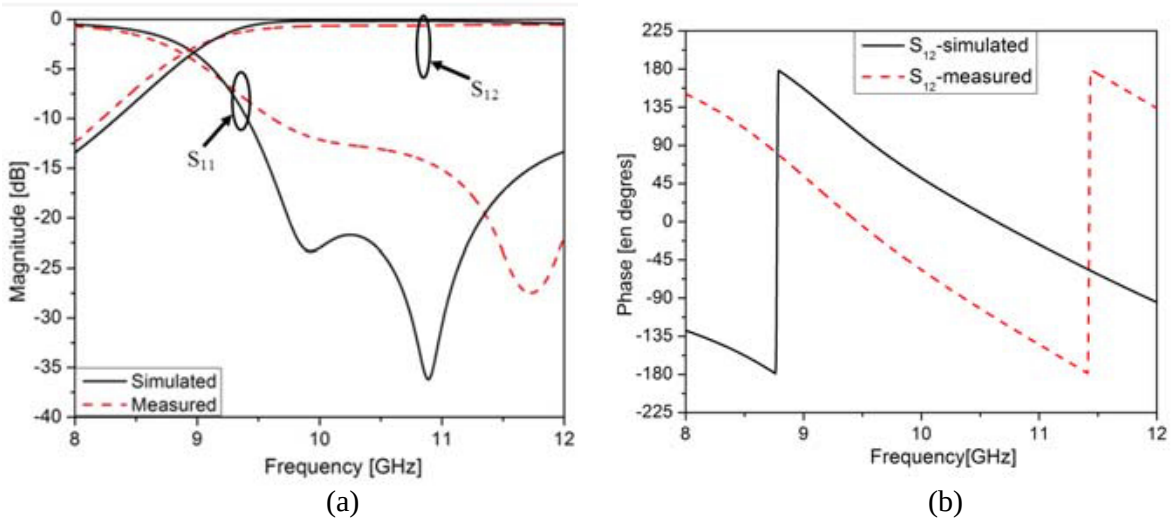

Figure 8. Simulated and measured S-parameters of the 45° phase shifter, (a) magnitudes of S_{11} and S_{12} for 45° phase shifter, (b) phase of S_{11} and S_{12} for 45° phase shifter.

A comparison of this work with [17] is presented in Table 3 in terms of bandwidth and size. It is observed that a significant reduction of 30% in terms of size and an increase of 0.4% of the bandwidth are achieved.

Table 3. Size and bandwidth between in the present work and in Reference [17].

Parameter	Present work	[17]	Significance
Size	15.7 mm × 27.6 mm	15.7 mm × 35 mm	30% reduction
Phase bandwidth ($\phi \pm 3°$)	0.7%	0.3%	0.4% improvement

3. NUMERICAL AND EXPERIMENTAL ANALYSIS OF THE FULL MATRIX

The proposed 4 × 4 Butler matrix uses four SIW couplers, two crossovers of via transitions connected with two SIW 45° phase shifters. It is fabricated on stacked printed circuit boards (PCBs) as shown in Fig. 9. The top PCB is coupled to the bottom PCB through the vias-transition (crossover). The Butler matrix has four inputs named $1R$, $2L$, $2R$, and $1L$, and four outputs A_1, A_2, A_3, and A_4, which are also represented as input ports 1, 2, 3, and 4 and output ports 5, 6, 7, and 8. The four outputs are used as inputs to antenna elements to produce four different radiation beams. The designed crossover introduces a non-zero phase difference between input 1 and output 2 (or input 4 and output 3) This additional phase is compensated through a delay line (L_{rc}) in the Butler matrix such that: $\Delta\varphi = \Delta\varphi_1 - \Delta\varphi_2 = 45°$, where $\Delta\varphi_1$ is the phase due to the phase shifter, and $\Delta\varphi_2$ is the phase due to the crossover. The dimensions of the Butler matrix are optimized for a frequency range around 10 GHz, and they are $L_m = 139$ mm (about $6\lambda_g$ at 10 GHz), $W_m = 93$ mm (about $4\lambda_g$ at 10 GHz), $\Delta\varphi = 45°$, and $L_{rc} = 1.06$ mm.

The simulated and measured S parameters of the Butler matrix are shown in Figs. 10 and 11, respectively. Simulated and measured insertion losses are, at 10 GHz, around 1.4 dB and 4.4 dB, respectively. Simulated and measured reflection coefficients are bellow −15 dB, from 9.5 GHz to 11.5 GHz. The differences observed in experimental insertion loss and return loss parameters in comparison with the simulations can be caused by the added connectors and fabrication tolerances. The experimental results could be improved by including the connectors and their real parameters in the simulations during the optimisation of the transitions between the connectors and microstrip lines.

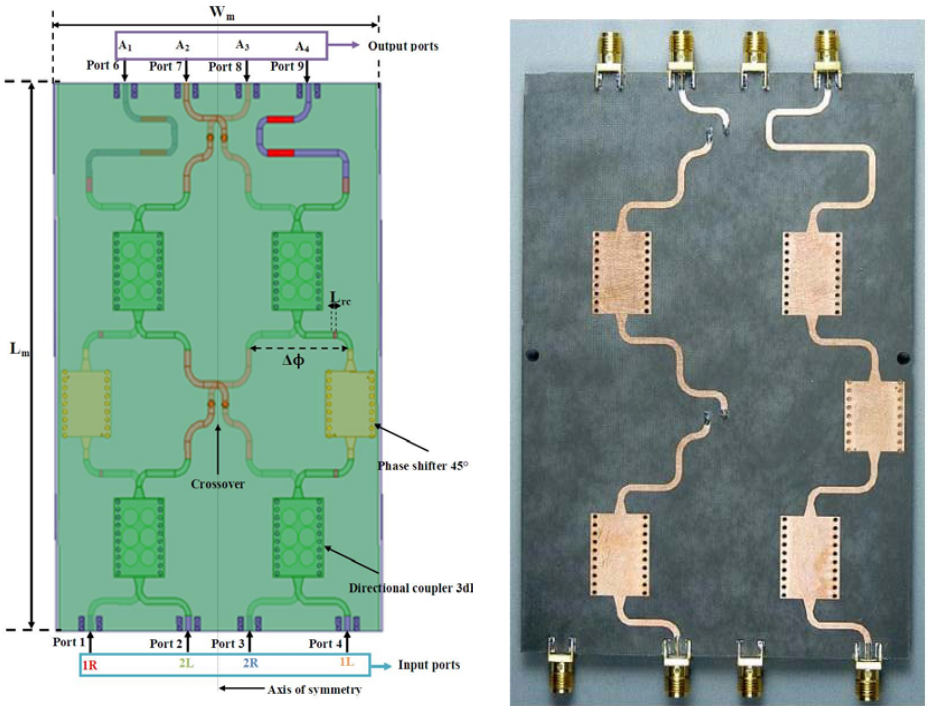

Figure 9. Structure of the proposed 4×4 Butler matrix. Fabricated 4×4 Butler matrix 4×4.

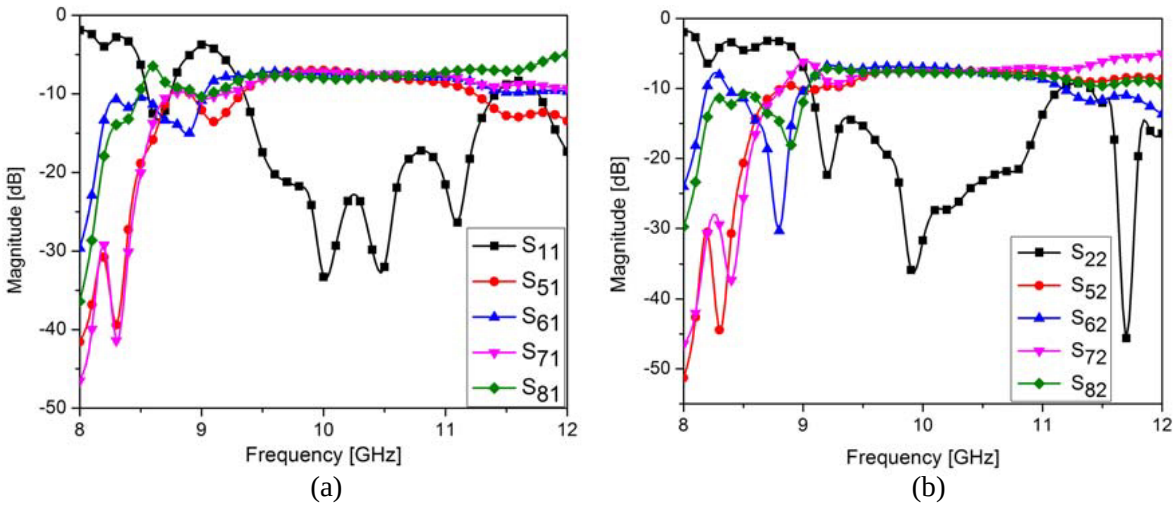

Figure 10. Simulated S parameters for 4×4 Butler matrix.

Table 4 summarizes the measured results of the corresponding phase shifts between the inputs and outputs for the proposed Butler matrix at 10 GHz. When the current is excited at any input port, the phase difference between adjacent output ports will only have one constant (β) as shown in Table 5. When the incoming signal is fed at input ports 1, 2, 3, and 4, the theoretical relative phase progression (β) between adjacent output ports should be $-45°$, $+135°$, $-135°$, and $+45°$, respectively. The measured phase differences between different output ports when the signal is fed at input ports are $-45° \pm 8°$, $135° \pm 10°$, $-135° \pm 6°$, and $45° \pm 6°$, respectively. This degradation could be due to fabrication tolerance and tolerance in dielectric constant of the substrate. However, the achieved performances are acceptable for X-band applications.

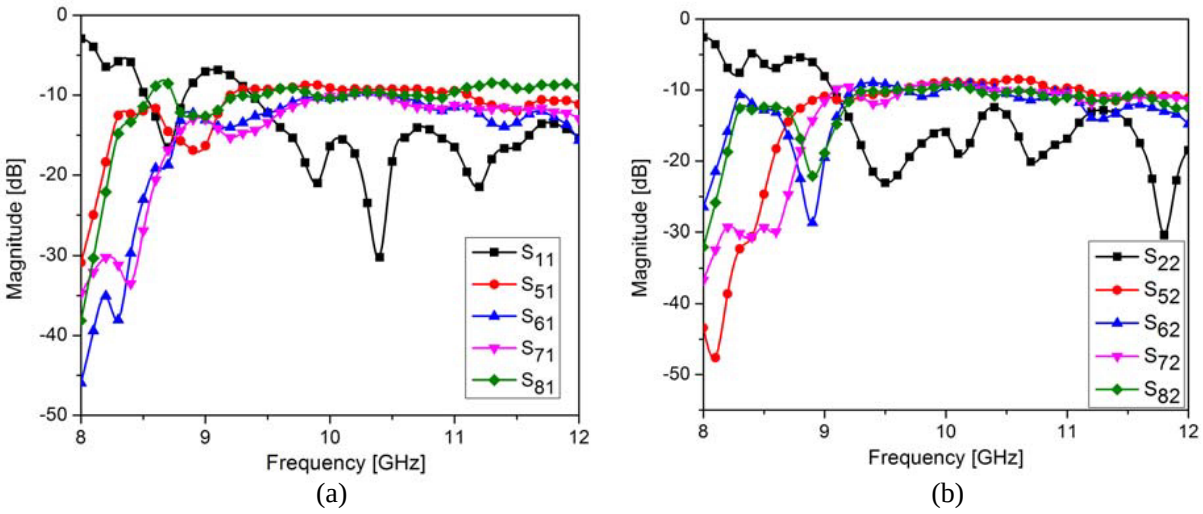

Figure 11. Measured insertion and return loss plots for 4×4 Butler matrix.

Table 4. Measured results of the phase shifts between the inputs and the outputs of the Butler matrix.

Ports	A_1	A_2	A_3	A_4
1R	$+173.25°$	$+136.59°$	$+94.05°$	$+51.58°$
2L	$+91.19°$	$-127.48°$	$+13.74°$	$+138.3°$
2R	$+135.56°$	$+3.85°$	$-132.56°$	$+85.89°$
1L	$+53.58°$	$+99.4°$	$+138.5°$	$-172.5°$

Table 5. Computed measured phase error.

Ports	$\beta_1 = A_2 - A_1$	$\beta_2 = A_3 - A_2$	$\beta_3 = A_4 - A_3$	Target
$1R$	$-36.66°$	$-42.55°$	$-42.47°$	$-45°$
|Error|	$8.34°$	$2.45°$	$2.53°$	
$2L$	$+141.33°$	$+141.22°$	$+124.56°$	$+135°$
|Error|	$6.33°$	$6.22°$	$10.44°$	
$2R$	$-131.71°$	$-136.41°$	$-141.55°$	$-135°$
|Error|	$3.29°$	$1.41°$	$6.55°$	
$1L$	$+45.82°$	$+39.1°$	$+49°$	$+45°$
|Error|	$0.82°$	$5.9°$	$4°$	

4. SIW ANTENNA ARRAY

A SIW based 4-element antenna array as presented in Fig. 12 was designed. To minimize the effect of mutual coupling between the elements and to ensure a low secondary lobe level, the ideal choice of the separation between the antenna elements is taken as $\lambda_0/2$.

The coupling coefficient between two adjacent ports is plotted in Fig. 13(a). The mutual coupling is below -15 dB in simulation, while in the measurement, it is below -20 dB in the desired X-band range. The measured and simulated return loss plots are in close agreement for the proposed antenna array as shown in Fig. 13(b).

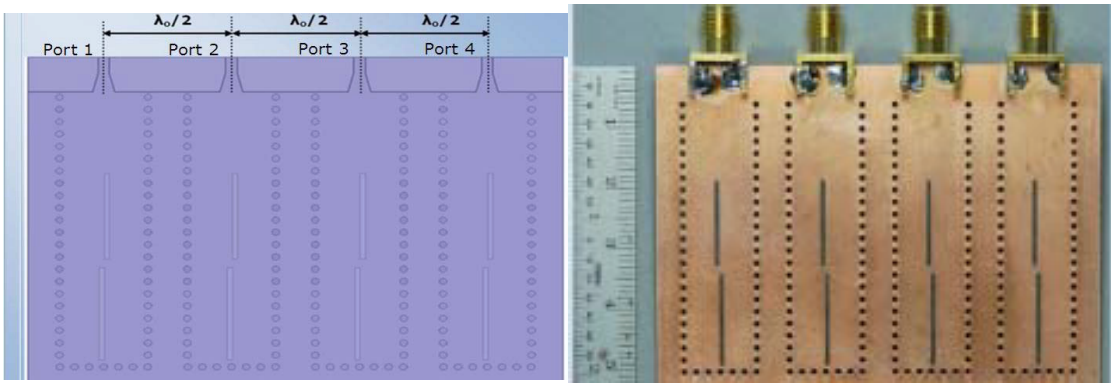

(a) (b)

Figure 12. (a) Proposed antenna array layout. (b) Photograph of the fabricated dual-slot linear antenna array.

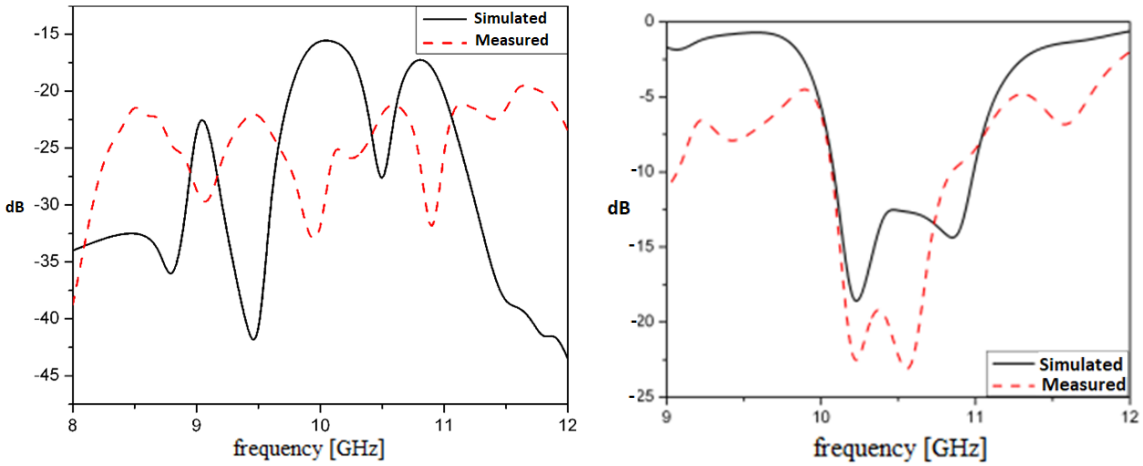

(a) (b)

Figure 13. (a) Coupling factor between two elements of the antenna array. (b) Return loss of the antenna array.

5. MULTI-BEAM ANTENNA

A schematic layout of the integrated dual-slot linear antenna array with the proposed Butler matrix is presented in Fig. 14, and the optimized dimensions of the antenna array are presented in Table 6. Four beams should be theoretically produced at $-45°$, $-15°$, $15°$, and $45°$ with their radiation patterns in the H-plane of the array at 10 GHz. Fig. 15 shows the simulated and measured radiation patterns of the multi-beam antenna in H plane, for different input ports. The antenna generates four beams oriented in the following directions: $-45°$, $-15°$, $15°$, and $45°$. In the radiation diagrams, variation in the level and number of secondary lobes are due to phase errors between different output ports.

The overall measured results are acceptable, and the four beams have an offset between $2°$ and $15°$. The main beam directions measured at 10 GHz are: $-11.25°$ ($1L$), $-30°$ ($2L$), $+15°$ ($1R$), and $+42°$ ($2R$). The side lobes of the $1L$ and $2L$ beams are below -5 dBi and 0 dBi, respectively. For other $2L$ and $2R$ ports, the side lobes are below 5 dBi. A good agreement can be observed between simulated and measured results.

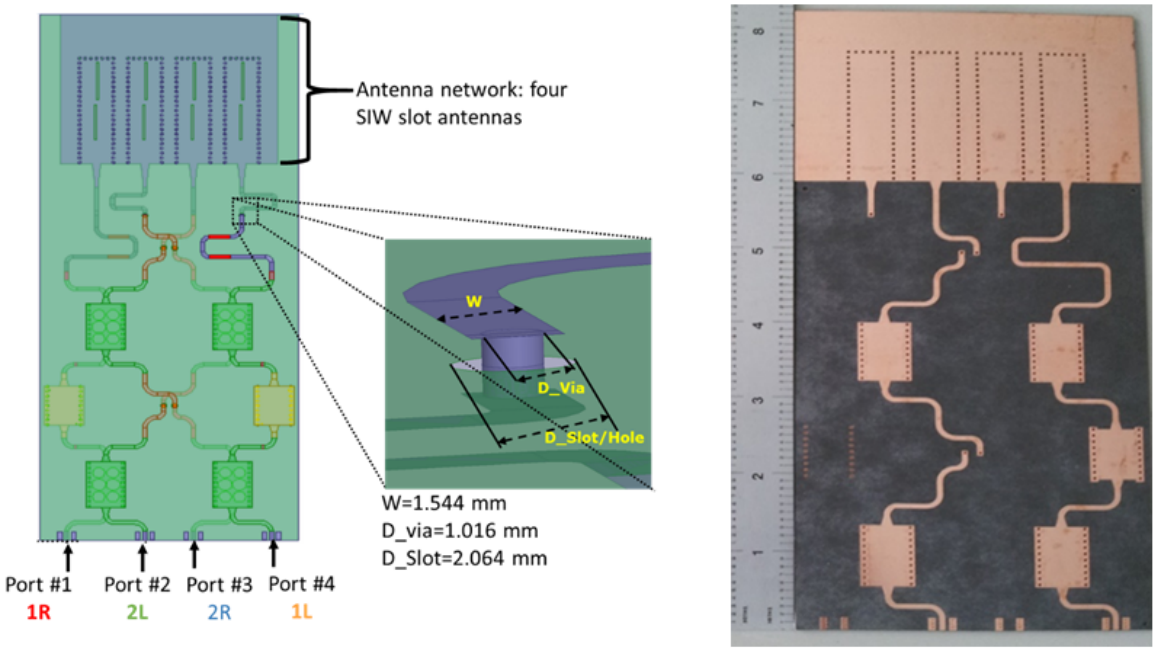

Figure 14. Schematic and photo of integrated dual-slot antenna array with the proposed Butler matrix.

Table 6. Dimensions of a proposed multi-beam antenna array.

L_{mb}	L_{ra}	W	D_{via}	D_{Slot}
76,86 mm	74,1 mm	1,544 mm	1,016 mm	2,064 mm

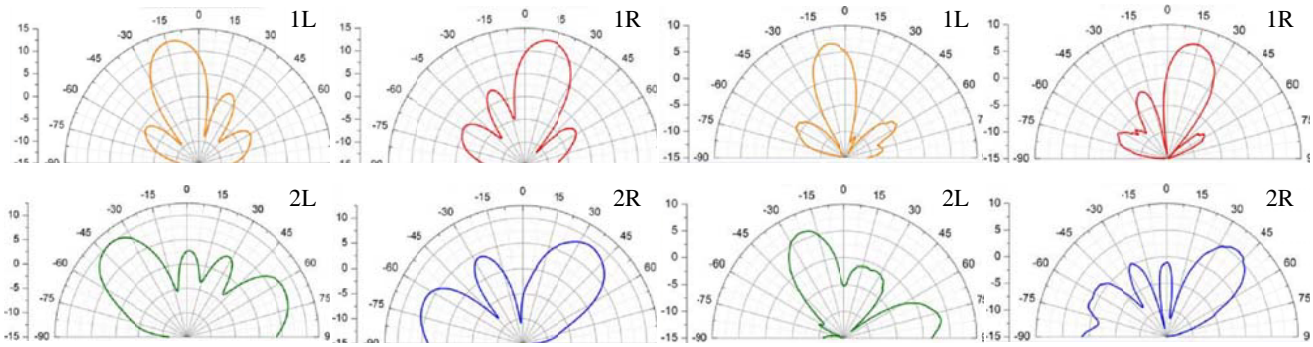

Figure 15. Radiation patterns at 10 GHz for the different input ports: (a) simulated and (b) measured results.

6. CONCLUSION

In this work, a novel 4×4 Butler matrix has been proposed for X-band applications. Prototypes of the different components and of the full structure have been designed, fabricated, and tested. The measured results are in good agreement with the simulated ones in terms of magnitudes of S-parameters and of phase shifts. A dual-slot antenna array has been integrated with the proposed matrix to form a multi-beam antenna, resulting in four different beam directions. Measured radiation patterns agree well with the theoretical predictions, validating the proposed work. The proposed Butler matrix is suitable for satellite communication systems operating in X-band.

REFERENCES

1. Hall, P. S. and S. J. Vetterlein, "Review of radio frequency beamforming techniques for scanned and multiple beam antennas," *IEE Proc.*, Vol. 137, No. 5, 293–303, 1990.
2. El-Zooghby, A., "Potentials of smart antennas in CDMA systems and uplink improvements," *IEEE Antennas Propag. Mag.*, Vol. 43, No. 5, 172–177, Oct. 2001.
3. Egami, S. and M. Kawai, "An adaptive multiple beam system concepts," *IEEE Journal on Selected Areas in Communications*, Vol. 5, No. 4, 630–636, May 1987.
4. Rotman, W. and R. Turner, "Wide-angle microwave lens for line source applications," *IEEE Trans. Antennas Propag.*, Vol. 11, No. 6, 623–632, Nov. 1963.
5. Shelton, J. P., "Focusing characteristics of symmetrically configured bootlace lenses," *IEEE Trans. Antennas Propag.*, Vol. 26, No. 4, 513–518, Jul. 1978.
6. Herd, J. S. and D. M. Pozar, "Design of a microstrip antenna array fed by a Rotman lens," *IEEE AP-S International Symposium*, Vol. 22, 729–732, Jun. 1984.
7. Blass, J., "Multi-directional antenna: New approach top stacked beams," *IRE Int. Convention Record*, 48–50, 1960.
8. Nolen, J., "Synthesis of multiple-beam networks for arbitrary illuminations," Ph.D. dissertation, Bendix Corporation, Radio Division, Baltimore, MD, Apr. 1965.
9. Butler, J. and R. Lowe, "Beam-forming matrix simplifies the design of electrically scanned antennas," *Electron Design*, 170–173, 1961.
10. White, W., "Pattern limitations in multiple-beam antennas," *IRE Trans. Antennas Propag.*, Vol. 10, 430–436, Jul. 1962.
11. Djerafi, T. and K. Wu, "A low-cost wideband 77-GHz planar Butler matrix in SIW technology," *IEEE Trans. Antennas Propag.*, Vol. 60, No. 10, 4949–4954, Oct. 2012.
12. Cheng, Y. J., C. A. Zhang, and Y. Fan, "Miniaturized multilayer folded substrate integrated waveguide Butler matrix," *Progress In Electromagnetics Research C*, Vol. 21, 45–58, 2011
13. Djerafi, T. and K. Wu, "Multilayered substrate integrated waveguide 4×4 Butler matrix," *Int. J. RF Microw. Comput.-Aided Eng.*, Vol. 22, No. 3, 336–344, Feb. 2012.
14. Yang, Q., Y. Ban, J. Lian, Z. Yu, and B. Wu, "SIW Butler matrix with modified hybrid coupler for slot antenna array," *IEEE Access*, Vol. 4, 9561–9569, 2016.
15. Lian, J., Y. Ban, Y. Wu, and L. Zhong, "Miniaturized multibeam array antenna based on E-plane Butler matrix for 5G application," *2018 IEEE International Symposium on Antennas and Propagation & USNC/URSI National Radio Science Meeting*, 1031–1032, 2018.
16. Mbaye, M., L. Talbi, K. Hettak, and A. Kabiri, "Design of 15 dB directional coupler using substrate integrated waveguide technology," *Microwave Opt. Technol. Lett.*, Vol. 54, 970–973, Apr. 2012.
17. Sellal, K., L. Talbi, T. A. Denidni, and J. Lebel, "Design and implementation of a substrate integrated waveguide phase shifter," *IET Microw. Antennas Propag.*, Vol. 2, No. 2, 194–199, Mar. 2008.